Nano Res (2009) 2: 321–326
DOI 10.1007/s12274-009-9029-4
Research Article

Synthesis of Vertically Oriented GaN Nanowires on a $LiAlO_2$ Substrate via Chemical Vapor Deposition

Xiaoli He, Guowen Meng (✉), Xiaoguang Zhu, and Mingguang Kong

Key Laboratory of Materials Physics, and Anhui Key Laboratory of Nanomaterials and Nanostructures, Institute of Solid State Physics, Chinese Academy of Sciences, Hefei 230031, China

Received: 21 June 2008 / Revised: 24 January 2009 / Accepted: 8 February 2009
©Tsinghua University Press and Springer-Verlag 2009. This article is published with open access at Springerlink.com

ABSTRACT

Vertically oriented nanowires (NWs) of single-crystalline wurtzite GaN have been fabricated on a γ-$LiAlO_2$ (100) substrate coated with a Au layer, via a chemical vapor deposition process at 1000 °C using gallium and ammonia as source materials. The GaN NWs grow along the nonpolar [10$\bar{1}$0] direction with steeply tapering tips, and have triangular cross-sections with widths of 50–100 nm and lengths of up to several microns. The GaN NWs are formed by a vapor–liquid–solid growth mechanism and the tapering tips are attributed to the temperature decrease in the final stage of the synthesis process. The aligned GaN NWs show blue-yellow emission originating from defect levels, residual impurities or surface states of the GaN NWs, and have potential applications in nanotechnology.

KEYWORDS

GaN, $LiAlO_2$, chemical vapor deposition, triangular cross-section, vapor–liquid–solid, photoluminescence

Introduction

One-dimensional single-crystalline semiconductor nanostructures are emerging as versatile nanoscale building blocks for future nanotechnologies [1–3]. GaN, a robust wide bandgap semiconductor, is an attractive candidate for use in high power optoelectronic devices due to its high melting point, high carrier mobility, and high electronic breakdown field [4]. Single-crystalline GaN nanowires (NWs) have shown promise in photonic and biological nanodevices, such as low power field-effect transistors (FET) [5], ultraviolet nanolasers [6, 7], and light-emitting diodes [8]. Moreover, well-aligned NWs have attracted great interest because they can be incorporated into devices and the individual NWs can be readily probed [9]. Hence, well-aligned GaN NWs have been the focus of extensive research [10–14]. Various methods have been developed for the synthesis of aligned GaN NWs, such as template-assisted synthesis [10], metal-organic chemical vapor deposition [11–13], and hydride vapor phase epitaxy [14]. However, all these synthetic schemes are either complicated or have high cost. According to Kuykendall et al. [12], specific substrate-based catalytic growth is feasible for NW arrays where there is symmetry and lattice constant match between the substrate and the GaN NWs. As the lattice mismatch

Address correspondence to gwmeng@issp.ac.cn

Springer

between γ-$LiAlO_2$ and GaN is relatively small (~1.4%) for the epitaxial relationship $(100)_{LiAlO_2}//(100)_{GaN}$, we chose single-crystal γ-$LiAlO_2$ (100) as the substrate for the growth of GaN NWs. We utilized chemical vapor deposition (CVD) to synthesize large-scale vertically oriented single-crystal GaN NWs with extremely tapering tips on a γ-$LiAlO_2$ (100) substrate coated with a layer of Au as catalyst. As the current and threshold voltage of NW-based FET devices are greatly influenced by the morphology of the NW apexes, the presence of sharp apexes in these NWs enlarges the electron tunneling probability, which is known to favor the field emission properties [15–20]. As it has been reported that well-aligned ZnO NWs with tiny tips can be used in a nanoscale negative ion generator [21], GaN NWs with such extremely tapering tips might also be introduced into this kind of negative ion generator.

Photoluminescence (PL) spectroscopy of the aligned GaN NWs shows blue–yellow emission originating from defect levels, residual impurities or surface states. These aligned GaN NWs with their tapering tips have potential applications in nanotechnology.

1. Experimental

Vertically aligned GaN NWs were synthesized on a γ-$LiAlO_2$ (100) substrate by a CVD process. A layer of Au catalyst (5 nm thick) was thermally evaporated onto a single-crystal γ-$LiAlO_2$ (100) substrate. Metallic Ga and ammonia were used as Ga and N precursors, respectively. As shown in Fig. 1, metal Ga was positioned in a quartz tube furnace, with the single-crystal γ-$LiAlO_2$ (100) substrate located about 5 mm above. The tube furnace was evacuated and flushed with NH_3, and then ramped at 40 °C/min to the growth temperature (1000 °C) in a flowing NH_3 atmosphere (25–28 sccm, standard cubic centimeters per minute). The furnace was kept at the growth temperature for 15 min before being cooled down. For comparison, a similar experimental procedure was performed to grow GaN NWs on a Si (100) substrate. The morphology, composition, and structure of the as-synthesized products were characterized by scanning electron microscopy (SEM, Sirion 200), transmission electron microscopy (TEM), and high-resolution TEM (JEOL-2010) equipped with an energy dispersive X-ray spectroscope (EDS) and X-ray diffractometry (XRD, X'Pert Pro MPD). Room temperature PL spectra were obtained by using a He-Cd laser under excitation of 325 nm.

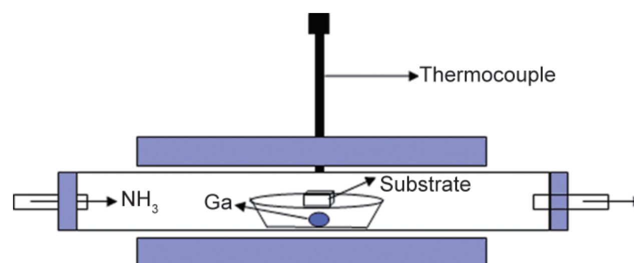

Figure 1 Apparatus for the synthesis of GaN NWs on a γ-$LiAlO_2$ (100) substrate

2. Results and discussion

SEM micrographs (Figs. 2 (a) and 2 (b)) of the products grown on the Au-coated γ-$LiAlO_2$ (100) substrate reveal a large quantity of vertically aligned NWs with symmetry-matched isosceles cross-sections. The widths measured along the base of the triangles are 50–200 nm, and the lengths of the NWs are several microns. From the inset of Fig. 2 (a), it can be seen that each NW consists of two parts, the bottom body part having a large diameter, and the top part having a tapering tip with a spherical gold particle on the end, indicating that the GaN NWs grow via a vapor–liquid–solid (VLS) mechanism. However, the GaN NWs grown on the Si (100) substrate under similar conditions are irregular and randomly distributed (Fig. 2 (c)).

X-ray diffraction (XRD) patterns of the GaN NWs grown on γ-$LiAlO_2$ and Si substrates are shown in Fig. 2 (d). All the peaks can be indexed to the hexagonal wurtzite structure of GaN with lattice constants of $a = 0.319$ nm and $c = 0.519$ nm. No diffraction peaks from impurities are found in the samples, implying that the products are hexagonal wurtzite GaN with high purity. Compared with the peaks of GaN NWs grown on the Si substrate, the (100) reflection peak of GaN NWs grown on the γ-$LiAlO_2$ substrate shows a marked increase in intensity, indicating that the GaN

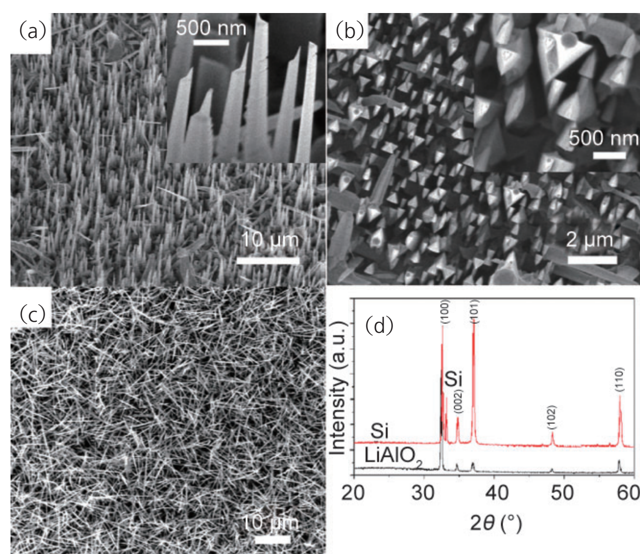

Figure 2 (a), (b) Top view SEM images of GaN NWs grown on a γ-$LiAlO_2$ (100) substrate, with magnified views in the insets; (c) top view SEM image of disordered GaN NWs grown on a Si (100) substrate; (d) XRD patterns of the GaN NWs grown on γ-$LiAlO_2$ and Si substrates, showing the hexagonal wurtzite structure of GaN and a preferential $[10\bar{1}0]$ growth direction for the sample on γ-$LiAlO_2$

NWs on the latter substrate grow preferentially along the $[10\bar{1}0]$ direction.

Further structural characterization of the NWs was performed by using TEM and high-resolution TEM (HRTEM). Figure 3 (a) shows an HRTEM image taken from the body part of the GaN NW (see the upper-left inset) with a width about 200 nm and the corresponding selected area electron diffraction (SAED) pattern (lower-left inset), revealing its single-crystalline nature. From the alignment of the HRTEM image and the diffraction pattern, the GaN NW clearly grows along the $[10\bar{1}0]$ direction, by stacking of nonpolar $[10\bar{1}0]$ planes of GaN, consistent with the XRD results. The interplanar spacings (d) of the GaN NW measured from the HRTEM image are about 0.275 and 0.515 nm for the $[10\bar{1}0]$ and (0001) planes, respectively. EDS measurements on the body part marked with a circle (Fig. 3 (c)) further confirm that the composition of the body part contains Ga and N with an approximate atomic ratio of 1:1. Therefore, the body part of the GaN NWs grown on the γ-$LiAlO_2$ substrates is clearly composed of aligned single-crystalline GaN NWs.

A tapering needle-like tip with catalyst particle on top is also observed by TEM, as shown in Fig. 3 (b). This needle-like tip with a diameter about 60 nm has a similar structure to the NW body part, with the same $[10\bar{1}0]$ growth direction and d-spacing of

(a) (b)

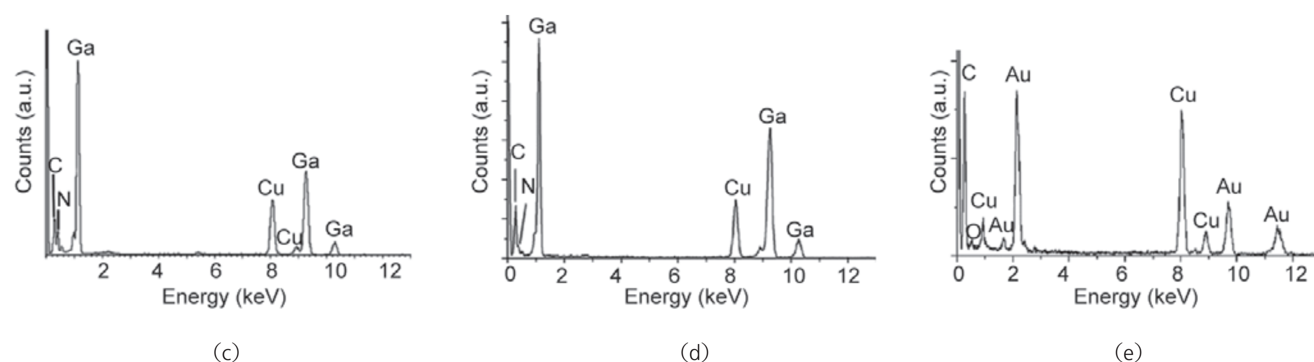

Figure 3 (a) HRTEM image of the body part of the GaN NW grown on the γ-$LiAlO_2$ substrate, with a TEM image shown in the upper-left inset and the corresponding SAED pattern in the the lower-left inset; (b) HRTEM image of a typical tapering tip part of GaN NWs, with the TEM image in the upper-left inset showing a Au catalyst droplet on its apex and the lower-left inset the corresponding SAED pattern taken from the tip part; (c), (d), (e) typical EDS spectra of the NWs taken from the circled areas marked as follows: (c) body part marked in (a), (d) tip part close to the Au catalyst marked in (b), and (e) Au catalyst droplet at the apex marked in (b)

0.281 nm for the (10$\bar{1}$0) plane. The single-crystalline characteristics of the wurtzite type hexagonal GaN can also be distinguished in the inset SAED pattern. However, the ratio of Ga and N about 7:1 (Fig. 3 (d)) is much higher than that in the body part (about 1:1). Figure 3 (e) shows an EDS spectrum recorded on the circled area of the darker contrast region in Fig. 3 (b), confirming the presence of the Au droplet on the NW tip in the upper-left inset.

The lattice and symmetry matching of GaN NWs with isosceles triangle cross-section morphology grown on γ-$LiAlO_2$ has previously been reported [11, 12]. As shown in Figs. 4 (a) and 4 (b), the lattice constants a=0.517 nm and c=0.628 nm of γ-$LiAlO_2$ closely match the lattice constant c (0.519 nm) and twice the lattice constant a (0.319 nm) of GaN, respectively [12]. Both the oxygen sublattice of γ-$LiAlO_2$ (100) plane and the wurtzite GaN (10$\bar{1}$0) plane have a matching two-fold symmetry. In fact, the well-matched isosceles triangle frames in Figs. 4(a) and 4(b) correctly predict the orientation of the GaN crystal plane at the interface, and show that the triangular cross-section is a manifestation of the two-fold symmetry along the [10$\bar{1}$0] crystallographic direction [12]. This symmetry match also determines the high degree of alignment of individual GaN NWs [9].

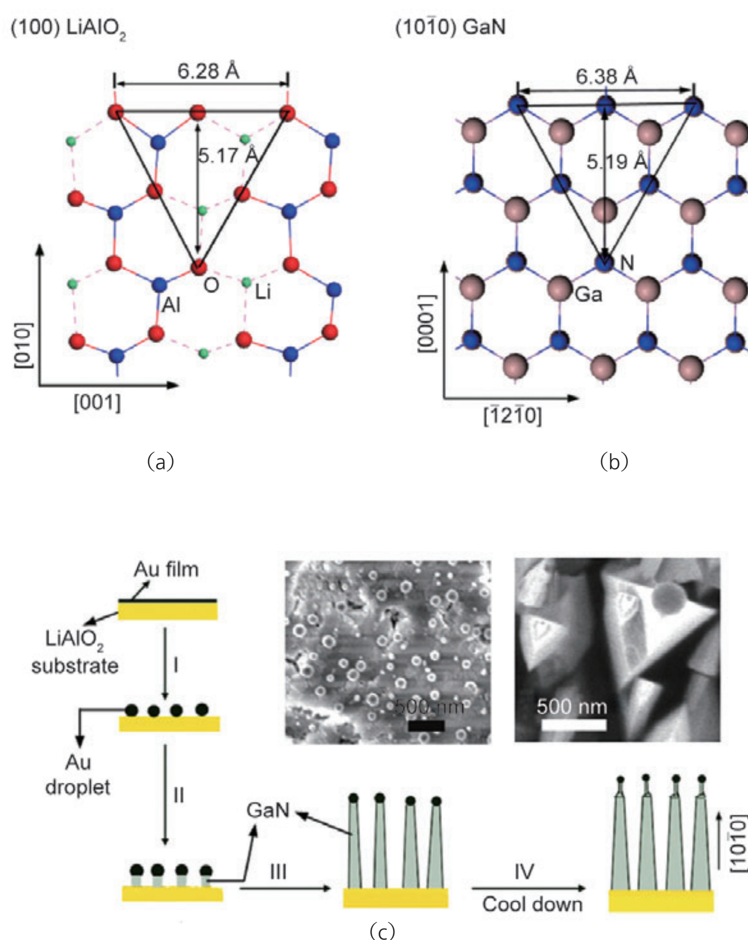

Figure 4 Schematic model illustrating the GaN NW growth: (a), (b) epitaxial relationship for GaN NWs with triangular cross-section grown on the γ-$LiAlO_2$ (100) plane; (c) the growth mechanism for GaN NWs with tapering needle-like tips. The inset SEM image (1) shows Au nanodroplets obtained by annealing the Au-coated $LiAlO_2$ substrate at 1000 °C in the absence of the Ga precursor, and the top view SEM image (2) of the GaN NWs clearly displays the triangular cross-sections

A model has been established to describe the growth process of the GaN NWs, as shown schematically in Fig. 4(c). As confirmed previously, a Au catalyzed VLS mechanism is responsible for the GaN NWs growth. At high temperature, the Au film breaks up into liquid Au nanodroplets on the surface of the γ-$LiAlO_2$ substrate, as demonstrated by the SEM image (inset (1) in Fig. 4(c)) (Process Ⅰ). The vaporized Ga atoms or molecules are subsequently absorbed by Au nanodroplets [9, 22]. The continuous absorption of Ga results in supersaturation and nucleation on the interface of the Au–Ga liquid alloys (Process Ⅱ). Subsequently, the nucleated Ga reacts with NH_3 with the assistance of Au as catalyst, leading to the continuous growth of GaN NWs, as described in Process Ⅲ. After growth of the GaN NWs for 15 min at 1000 °C, the furnace was cooled down in the presence of flowing ammonia (Process Ⅳ). In this case, tapering needle-like tips (see the SEM image in inset (2) in Fig. 4 (c)) are formed in Process Ⅳ with a plentiful supply of ammonia. Based on the large difference in Ga/N ratio between the body part (1:1) and tip part (7:1), we suggest that the decrease in temperature plays a key role in the formation of the tapering needle-like tips. As the temperature decreases rapidly from 1000 °C to 600 °C in several minutes, the rate of decomposition of

NH_3 is significantly reduced while the number of Ga atoms dissolved in the catalyst decreases only slightly, resulting in much higher Ga/N ratio (7:1) in the tip parts. Simultaneously, the decreasing temperature inhibits the migration of most of the precipitated Ga atoms and restricts their growth to the tip apexes. As the temperature drops further, Ga evaporation is restricted, which reduces the Ga absorption by Au droplets and any further separation. Thus, the tapering needle-like tips form with a high Ga/N ratio.

A typical room temperature PL spectrum for the aligned GaN NWs on the γ-$LiAlO_2$ substrate, illustrated in Fig. 5, shows two broad emission peaks at about 390 nm and 532 nm. The weaker blue emission peak at 390 nm can be attributed to the transition from a shallow donor state to a shallow acceptor state involving defect levels or residual impurities [22, 23]. The peak at 532 nm corresponds to the well-known "yellow" emission band associated with the existence of defect or surface states [24, 25]. It should be noted that the near band emission of GaN cannot be observed, which may result from overlap with the broad blue emission peak at 390 nm. The PL spectrum was measured from the top of the NWs where the tapering needle-like tips with a Ga/N ratio of 7:1 are exposed to the laser, which probably leads to an increased number of defects or surface states.

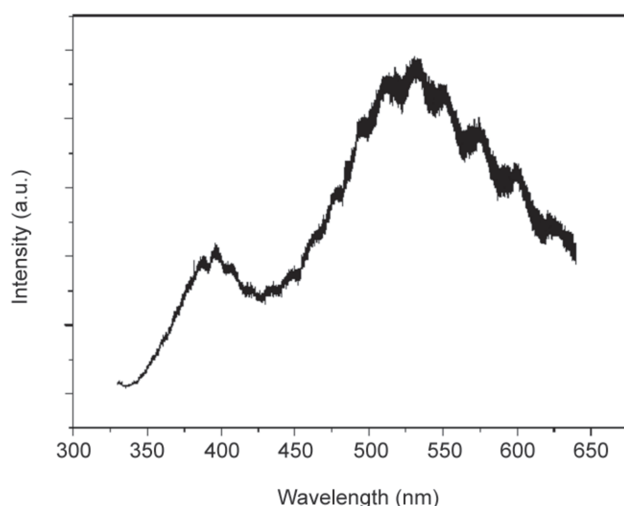

Figure 5 Room temperature photoluminescence spectrum of the GaN NWs grown on the γ-$LiAlO_2$ substrate

3. Conclusions

As a result of the symmetry match and small lattice constant mismatch between$(100)_{LiAlO_2}//(100)_{GaN}$, vertically oriented single-crystalline wurtzite GaN NWs, with symmetry-matched isosceles cross-sections and extremely tapering needle-like tips, have been synthesized on a Au-coated γ-$LiAlO_2$ (100) substrate in a CVD process via the reaction of Ga and ammonia at 1000 °C. The GaN NWs with widths of 50–100 nm and lengths of several microns grow along the non-polar $[10\bar{1}0]$ direction. The growth of GaN NWs follows the VLS mechanism and the formation of tapering tips can be attributed to the temperature decrease during the final growth period of the CVD process. The blue-yellow photoluminescence emission from GaN NWs can be ascribed to the formation of defects or surface states. The high degree of alignment of the GaN NWs together with their peculiar morphology may open up applications of these materials in future nanodevices.

Acknowledgements

We are grateful for the support of the National Natural Science Foundation of China (50525207 and 10374092) and the National Basic Research Program of China (2007CB936601).

References

[1] Xia, Y.; Yang, P.; Sun, Y.; Wu, Y.; Mayers, B.; Gates, B.; Yin, Y.; Kim, F.; Yan, H. One-dimensional nanostructures: Synthesis, characterization, and applications. *Adv. Mater.* **2003**, *15*, 353–389.

[2] Wang, J.; Gudiksen, M. S.; Duan, X.; Cui, Y.; Lieber, C. M. Highly polarized photoluminescence and photodetection from single indium phosphide nanowires. *Science* **2001**, *293*, 1455–1457.

[3] Law, M; Sirbuly, D. J.; Johnson, J. C.; Goldberger, J.; Saykally, R. J.; Yang, P. Nanoribbon waveguides for subwavelength photonics integration. *Science* **2004**, *305*, 1269–1273.

[4] Johnson, J. C.; Choi, H. -J.; Knutsen, K. P.; Schaller, R. D.; Yang, P.; Saykally, R. J. Single gallium nitride nanowire lasers. *Nat. Mater.* **2002**, *1*, 106–110.

[5] Huang, Y.; Duan, X.; Cui, Y.; Lieber, C. M. Gallium nitride nanowire nanodevices. *Nano Lett.* **2002**, *2*, 101–104.

[6] Gradečak, S.; Qian, F.; Li, Y.; Park, H. -G.; Lieber, C. M. GaN nanowire lasers with low lasing thresholds. *Appl. Phys. Lett.* **2005**, *87*, 173111.

[7] Pauzauskic, P. J.; Sirbuly, D. J.; Yang, P. Semiconductor nanowire ring resonator laser. *Phys. Rev. Lett.* **2006**, *96*, 143903.

[8] Kim, H. M.; Kang, T. W.; Chung, K. S. Nanoscale ultraviolet-light emitting diodes using wide-bandgap gallium nitride nanorods. *Adv. Mater.* **2003**, *15*, 567–569.

[9] Liu, B. D.; Bando, Y.; Tang, C. C.; Xu, F. F.; Golberg, D. Quasi-aligned single-crystalline GaN nanowire arrays. *Appl. Phys. Lett.* **2005**, *87*, 073106.

[10] Cheng, G. S.; Chen, S. H.; Zhu, X. G.; Mao, Y. Q.; Zhang, L. D. Highly ordered nanostructures of single-crystalline GaN nanowires in anodic alumina membranes. *Mater. Sci. Eng. A* **2000**, *286*, 165–168.

[11] Kuykendall, T.; Pauzauskie, P; Lee, S.; Zhang, Y.; Goldberger, J.; Yang, P. Metalorganic chemical vapor deposition route to GaN nanowires with triangular cross sections. *Nano Lett.* **2003**, *3*, 1063–1066.

[12] Kuykendall, T.; Pauzauskie, P. J.; Zhang, Y.; Goldberger, J.; Sirbuly, D.; Denlinger, J.; Yang, P. Crystallographic alignment of high-density gallium nitride nanowire arrays. *Nat. Mater.* **2004**, *3*, 524–528.

[13] Wang, X.; Sun, X.; Fairchild, M.; Hersee, S. D. Fabrication of GaN nanowire arrays by confined epitaxy. *Appl. Phys. Lett.* **2006**, *89*, 233115

[14] Kim, H. -M.; Kim, D. S.; Park, Y. S.; Kim, D. Y.; Kang, Chung, K. S. Growth of GaN nanorods by a hydride vapor phase epitaxy method. *Adv. Mater.* **2002**, *14*, 991 –993.

[15] Liu, B.; Yoshio, B.; Tang, C.; Xu, F.; Hu, J.; Dmitri, G. Needle-like bicrystalline GaN nanowires with excellent field emission properties. *J. Phys. Chem. B* **2005**, *109*, 17082–17085.

[16] Meng, X. Q.; Shen, D. Z.; Zhang, J. Y.; Zhao, D. X.; Dong, L.; Lu, Y. M.; Liu, Y. C.; Fan, X. W. Photoluminescence properties of catalyst-free growth of needle-like ZnO nanowires. *Nanotechnolgoy* **2005**, *16*, 609–612.

[17] Lai, W. H.; Hon, M. H.; Teoh, L. G.; Su, Y. H.; Shieh, J.; Chen, C. K. Field-emission performance of wormhole like mesoporous tungsten oxide nanowires. *J. Electron. Mater.* **2008**, *37*, 1082–1087.

[18] Min, Z. G.; Roy, E.; Wen, L. H.; Min, L. W.; Min, H. S.; Zhang K. Y.; Quan, X. Z. Field emission from an array of free-standing metallic nanowires. *Chin. Phys. Lett.* **2002**, *19*, 1016–1018.

[19] Simpkins, B. S.; Pehrsson, P. E.; Taheri, M. L.; Stroud, R. M. Diameter control of gallium nitride nanowires. *J. Appl. Phys.* **2007**, *101*, 094305.

[20] Zhou, J.; Gong, L.; Deng, S. Z.; Chen, J.; She, J. C.; Xu, N. S.; Yang, R.; Wang, Z. L. Growth and field-emission property of tungsten oxide nanotip arrays. *Appl. Phys. Lett.* **2005**, *87*, 223108.

[21] Chen, C. -H.; Huang, B. -R.; Lin, T. -S.; Chen, I. -C.; Hsu, C. -L. A new negative ion generator using ZnO nanowire array. *J. Electrochem. Soc.* **2006**, *153*, G894–G896.

[22] Biswas, S.; Kar, S.; Ghoshal, T.; Ashok, V. D.; Chakrabarti, S.; Chaudhuri, S. Fabrication of GaN nanowires and nanoribbons by a catalyst assisted vapor–liquid–solid process. *Mater. Res. Bull.* **2007**, *42*, 428–436.

[23] Chen, X.; Li, J.; Cao, Y.; Lan, Y.; Li, H.; He, M.; Wang, C.; Zhang, Z.; Qiao, Z. Straight and smooth GaN nanowires. *Adv. Mater.* **2000**, *12*, 1432–1434.

[24] Colton, J. S.; Yu, P. Y.; Teo, K. L.; Perlin, P.; Weber, E. R.; Grzegory, I.; Uchida, K. Selective excitation of the yellow luminescence of GaN. *Physica B* **1999**, 273–274, 75–79.

[25] Jiang, D. -S.; Zhao, D. -G.; Yang, H. Optical analysis of dislocation-related physical processes in GaN-based epilayers. *Phys. Status Solidi B* **2007**, *244*, 2878–2891.